IOP Publishing Physica Scripta
Phys. Scr. 95 (2020) 065224 (11pp) https://doi.org/10.1088/1402-4896/ab8800

Investigating the viscous damping effects on the propagation of Rayleigh waves in a three-layered inhomogeneous plate

Rahmatullah Ibrahim Nuruddeen[1,2], R Nawaz[1] and Q M Zaigham Zia[1]

[1] Department of Mathematics, COMSATS University Islamabad, Park Road, Chak Shahzad, Islamabad 44000, Pakistan
[2] Department of Mathematics, Faculty of Science, Federal University Dutse, Jigawa State, Nigeria

E-mail: NuruddeenRahmatullah.n@fud.edu.ng

Received 9 January 2020, revised 1 April 2020
Accepted for publication 8 April 2020
Published 16 April 2020

Abstract

The present paper investigates the propagation of anti-plane Rayleigh waves in an elastic three-layered inhomogeneous plate in the presence of viscous damping. The core layer is sandwiched between skin layers with appropriate perfect interfacial boundary conditions, while traction-free conditions are prescribed on the outer faces. The eigenfunctions expansion method is employed for the study. Various cases of damped and undamped situations have been examined in connection to the obtained displacements and shear stresses. Finally, the effects of viscous damping on the propagation of Rayleigh waves are reported graphically using some physical available data.

Keywords: layered inhomogeneous plate, rayleigh waves, viscous damping, eigenfunctions method

(Some figures may appear in colour only in the online journal)

1. Introduction

Wave propagation in elastic media is an important area in solid mechanics that continues to gain ground due its wide range of applications including the earthquake science, elastodynamics, geophysics, aerodynamics, and a lot of engineering branches, among others, [1–3]. In particular, a variety of studies have been carried out in regard to the wave propagation in elastic media consisting of periodic and graded waveguides [4, 5], laminated and composite elastic beams [6, 7] and layered plates [8–12] to mention a few. Of interest, layered plates including multilayered and composite structures play vital role in many physical applications leading to several investigations both experimentally and theoretically, [8–10]. In particular, a three-layered plate that is characterized by soft-stiff layers appears in many configurations depending on the application. For, instance, laminated glasses consists of thin soft core layer and stiff facings are used in glazing applications; photovoltaic panels are made of light core layer with stiff facings and used in solar energy; while the classical sandwich plates normally emerged with light core layer and stiff facings, with a variety of applications including in elastic beams [11, 12]. Mathematically, a quite number of studies have been reported in the literature in regard to layered plates comprising of the harmonic wave propagation in layered elastic sandwiches [11], elastic waves dispersion in three-layered plates [12], low-frequency motions of elastic multi-component structures [13], analysis of composite sandwich plates of a five-layered nature with viscoelastic cores [14] and the dynamicity of five-layered plates for various thicknesses made of glass material [15], see also [16–23] among others and the references therein. Besides, viscous damping effects in regards to propagation of elastic waves in layered media has not been found in the literature, of which is it believed to affect such propagation considerably.

However, the present paper examines the propagation of anti-plane Rayleigh waves in an isotropic three-layered inhomogeneous elastic plate in the presence of viscous damping. The core layer is sandwiched between skin layers with prescribed perfect interfacial conditions within and traction-free boundary conditions on the outer faces of the skin layers. Underlying is aimed to study damping effects on the propagation of Raleigh waves in a multiple layered plate and determine global estimates for lower eigenvalues, if any.

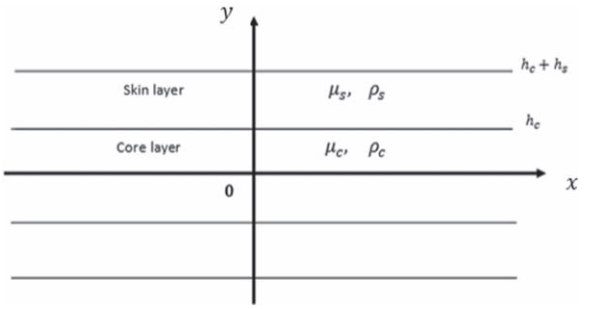

Figure 1. Symmetric inhomogeneous three-layered plate.

It is worth mentioning that global estimates of lower eigenvalues in the presence of damping help in further determining the optimal dispersion relations while considering different multilayered structures with material contrast setups, see [1, 12, 13]. The eigenfunctions expansion method is considered for the present investigation. Similarly, a numerical bisection method will be utilized to deal with the resulting transcendental eigenvalues equation. The displacements and stresses in the respective layers of the plate amidst the viscous damping corresponding to both the symmetric and antisymmetric motions will be determined. Various cases of free damped and undamped situations will be examined. Also, some physical data available in the literature will be sought for the numerical computations of the problem, and the results will be depicted graphically. Furthermore, the paper is arranged as follows: section 2 gives the formulation of the problem, and the solution of the problem is given in section 3. In section 4, analysis of the obtained solution is presented, while section 5 presents the numerical results and makes some discussions, and section 6 gives the concluding remarks.

2. Formulation of the problem

Consider an isotropic symmetric strongly inhomogeneous three-layered plate as shown in figure 1 below consisting of the upper skin layer $h_c \leqslant y \leqslant (h_c + h_s)$, the core layer $-h_c \leqslant y \leqslant h_c$ and the lower skin layer in $-(h_c + h_s) \leqslant y \leqslant -h_c$.

We then define an anti-plane dynamic problem by considering the classical equation of motion [1, 2, 24, 25] in the presence of viscous damping [26] given in Cartesian coordinates (x, y) as follows

$$\frac{\partial \sigma_{13}^q}{\partial x} + \frac{\partial \sigma_{23}^q}{\partial y} = \rho_q \frac{\partial^2 U^q}{\partial t^2} + \delta \frac{\partial U^q}{\partial t}, \quad t > 0, \quad q = c, s, \quad (1)$$

with the spatial variables x, y, the temporal variable t, and the out of plane displacements U^q for $q = c$ and $q = s$ standing for the core and skin layers, respectively. Also, ρ_q are the volume mass densities, δ is the viscous damping parameter, [26]. The stresses σ_{j3}^q, for $j = 1, 2$ are given by

$$\sigma_{13}^q = \mu_q \frac{\partial U^q}{\partial x}, \quad \sigma_{23}^q = \mu_q \frac{\partial U^q}{\partial y}, \quad q = c, s, \quad (2)$$

where μ_q are the Lame's elastic parameters. The prescribed continuity or interfacial conditions are as follows:

$$U^c(x, y, t) = U^s(x, y, t),$$
$$\sigma_{23}^c(x, y, t) = \sigma_{23}^s(x, y, t), \text{ at } y = \pm h_c, \ t > 0. \quad (3)$$

The traction-free conditions on the outer skin faces are given by:

$$\sigma_{23}^s(x, y, t) = 0, \text{ at } y = \pm(h_c + h_s), \ t > 0. \quad (4)$$

The initial conditions at $t = 0$ are also given to be:

$$U^q(x, y, 0) = F_q(x, y), \ U_t^q(x, y, 0) = G_q(x, y), \ q = c, s, \quad (5)$$

where $F_q(x, y)$ and $G_q(x, y)$ are given continuous functions in x, y. Thus, in view of the above formulated problem, we therefore aim in this paper to examine the displacements and stresses in the respective layers of the inhomogeneous plate under consideration by studying the effects of the viscous damping parameter in both the skin and core layers. The powerful analytical method called the eigenfunctions expansion method [27] is adopted for the investigation.

3. Solution method of the problem

To solve the direct solution of the formulated problem, we employ the eigenfunctions expansion method. However before then, due the missing boundary conditions x variable, we first convert the given problem in equations (1)–(5) to a system solvable by the above said method. In doing so, a kind of harmonic solution of the form:

$$U^q(x, y, t) = V^q(y, t)e^{ikx}, \quad q = c, s, \quad (6)$$

is assumed on x variable to satisfy the displacement field; where $i = \sqrt{-1}$, and k is the wave number. Thus, the initial conditions also take the following form from equation (6)

$$F_q(x, y) = f_q(y)e^{ikx}, \ G_q(x, y) = g_q(y)e^{ikx}, \quad q = c, s, \quad (7)$$

where $f_q(y)$ and $g_q(y)$ are continuous functions. Therefore, by virtue of the above assumption, equations (1)–(5) transform to the following system:

$$\frac{\partial^2 V^q}{\partial y^2} - k^2 V^q = \frac{1}{c_q^2}\frac{\partial^2 V^q}{\partial t^2} + \frac{\delta}{\mu_q}\frac{\partial V^q}{\partial t}, \ t > 0, \ q = c, s, \quad (8)$$

where $c_q = \sqrt{\frac{\mu_q}{\rho_q}}$, is the transverse speed. We also get the following continuity conditions as proceed:

$$V^c(y, t) = V^s(y, t), \quad \mu_c \frac{\partial V^c(y, t)}{\partial y} = \mu_s \frac{\partial V^s(y, t)}{\partial y}, \text{ at } y = \pm h_c, \ t > 0, \quad (9)$$

and the traction-free boundary conditions:

$$\frac{\partial V^s(y, t)}{\partial y} = 0, \text{ at } y = \pm(h_c + h_s), \ t > 0. \quad (10)$$

The initial conditions now take the form:

$$V^q(y, 0) = f_q(y), \quad V_t^q(y, 0) = g_q(y), \quad q = c, s. \tag{11}$$

Now, with the application of the eigenfunctions expansion method, let the solution of equation (8) take the following form

$$V^q(y, t) = \sum_{m=1}^{\infty} X_{qm}(y) T_{qm}(t), \quad q = c, s, \tag{12}$$

where $X_{qm}(y)$ are the eigenfunctions for $m = 1, 2, 3, \ldots$. Then, the corresponding spectral problem from equations (8)–(11) takes the following form:

$$\begin{cases} X''_{qm}(y) + (\lambda_m^2 - k^2) X_{qm}(y) = 0, \\ X_{cm}(y) = X_{sm}(y), \quad \mu_c X'_{cm}(y) = \mu_s X'_{sm}(y), \text{ at } y = \pm h_c, \\ X'_{sm}(y) = 0, \text{ at } y = \pm(h_c + h_s), \end{cases} \tag{13}$$

for $q = c, s$. More, from the above spectral problem, we get the respective solutions in the upper skin, core and lower skin layers as follows:

$$\begin{cases} X_{sm}(y) = A_1 \cos(y\sqrt{\lambda_m^2 - k^2}) + B_1 \sin(y\sqrt{\lambda_m^2 - k^2}), & h_c \leqslant y \leqslant (h_c + h_s), \\ X_{cm}(y) = A_2 \cos(y\sqrt{\lambda_m^2 - k^2}) + B_2 \sin(y\sqrt{\lambda_m^2 - k^2}), & -h_c \leqslant y \leqslant h_c, \\ X_{sm}(y) = A_3 \cos(y\sqrt{\lambda_m^2 - k^2}) + B_3 \sin(y\sqrt{\lambda_m^2 - k^2}), & -(h_c + h_s) \leqslant y \leqslant -h_c, \end{cases} \tag{14}$$

where A_l, B_l, $l = 1, 2, 3$ are constants to be determined. Now, since the structure is considered to be symmetrical about $x = 0$, we therefore analyze both the symmetric and anti-symmetric solutions of the governing problem in subsections below. In doing so, we obtain the expected eigenvalues and eigenfunctions, and the corresponding displacements and stresses in the respective layers of the plate.

3.1. Symmetric solutions

With the symmetric solution consideration for $y \geqslant 0$, equation (14) reduces to the following

$$\begin{cases} X_{cm}(y) = A_2 \cos(y\sqrt{\lambda_m^2 - k^2}), \\ X_{sm}(y) = A_1 \cos(y\sqrt{\lambda_m^2 - k^2}) + B_1 \sin(y\sqrt{\lambda_m^2 - k^2}), \end{cases} \tag{15}$$

and leading to the following solution matrix from the conditions given in equations (9)–(10)as follows:

$$\begin{pmatrix} \cos(h_c\sqrt{\lambda_m^2 - k^2}) & \sin(h_c\sqrt{\lambda_m^2 - k^2}) & -\cos(h_c\sqrt{\lambda_m^2 - k^2}) \\ -\sin(h_c\sqrt{\lambda_m^2 - k^2}) & \cos(h_c\sqrt{\lambda_m^2 - k^2}) & \frac{\mu_c}{\mu_s}\sin(h_c\sqrt{\lambda_m^2 - k^2}) \\ -\sin((h_c + h_s)\sqrt{\lambda_m^2 - k^2}) & \cos((h_c + h_s)\sqrt{\lambda_m^2 - k^2}) & 0 \end{pmatrix}, \tag{16}$$

that gives the following eigenwave equation

$$\cot(h_c\sqrt{\lambda_m^2 - k^2}) \tan(h_s\sqrt{\lambda_m^2 - k^2}) = -\frac{\mu_c}{\mu_s}. \tag{17}$$

Equation (17) cannot explicitly be solved for the eigenvalues λ_m analytically, but numerically or by other means [28]. Also, analyzing further for lower eigenvlues $\lambda_m \ll 1$, we set $k = 0$ in equation (17) and found that it does not have a global estimate for lower values of λ_m.

Also for the eigenfunctions, the solutions given in equation (15) via the conditions in equations (9)–(10)for $y \geqslant 0$ are revealed to be as follows:

$$\begin{cases} X_{cm}(y) = \cos(y\sqrt{\lambda_m^2 - k^2}), \\ X_{sm}(y) = A_{2m}(\cos(y\sqrt{\lambda_m^2 - k^2}) + \tan((h_c + h_s)\sqrt{\lambda_m^2 - k^2}) \sin(y\sqrt{\lambda_m^2 - k^2})), \end{cases} \tag{18}$$

where

$$A_{2m} = \frac{\cos(h_c\sqrt{\lambda_m^2 - k^2})}{\cos(h_c\sqrt{\lambda_m^2 - k^2}) + \sin(h_c\sqrt{\lambda_m^2 - k^2}) \tan((h_c + h_s)\sqrt{\lambda_m^2 - k^2})}. \tag{19}$$

Now, to determine the function $T_{qm}(t)$, we substitute equation (12) with the help of equation (13) into equation (8) and the initial conditions given in equation (11) to get the following differential equations:

$$\begin{cases} T''_{qm}(t) + \frac{\delta c_q^2}{\mu_q} T'_{qm}(t) + (c_q \lambda_m)^2 T_{qm}(t) = 0, \\ T_{qm}(0) = R_m, \quad T'_{qm}(0) = N_m, \end{cases} \tag{20}$$

for $q = c, s$, where R_m and N_m are given by the application of the Fourier's series as

$$R_m = \frac{\int_0^{h_c} f_c(\xi_2) X_{cm}(\xi_2) d\xi_2 + \int_{h_c}^{h_s} f_s(\xi_2) X_{sm}(\xi_2) d\xi_2}{\int_0^{h_c} X_{cm}^2(\xi_2) d\xi_2 + \int_{h_c}^{h_s} X_{sm}^2(\xi_2) d\xi_2},$$
$$N_m = \frac{\int_0^{h_c} g_c(\xi_2) X_{cm}(\xi_2) d\xi_2 + \int_{h_c}^{h_s} g_s(\xi_2) X_{sm}(\xi_2) d\xi_2}{\int_0^{h_c} X_{cm}^2(\xi_2) d\xi_2 + \int_{h_c}^{h_s} X_{sm}^2(\xi_2) d\xi_2}. \tag{21}$$

The solutions of equation (20) are given by

$$T_{qm}(t) = \frac{\alpha_m R_m \cosh\left(\frac{\alpha_m}{2\mu_q} t\right) + M_m \sinh\left(\frac{\alpha_m}{2\mu_q} t\right)}{\alpha_m} e^{-\frac{\delta c_q^2}{2\mu_q} t}, \tag{22}$$

where $M_m = 2\mu_q N_m + \delta c_q^2 R_m$ and $\alpha_m = \sqrt{c_q^4 \delta^2 - 4\mu_q c_q^2 \lambda_m^2}$.

Thus, from the assumptions made at the beginning of this section and via equations (6), (12) and (22) we get the complete out of plane displacements in the respective layers as

$$U^q(x, y, t) = \sum_{m=1}^{\infty} \left(\frac{\alpha_m R_m \cosh\left(\frac{\alpha_m}{2\mu_q} t\right) + M_m \sinh\left(\frac{\alpha_m}{2\mu_q} t\right)}{\alpha_m} \right) \times X_{qm}(y) e^{ikx - \frac{\delta c_q^2}{2\mu_q} t}, \quad q = c, s, \tag{23}$$

where $X_{qm}(y)$ for $q = c, s$ are given in equation (18), and R_m and N_m in equation (21).

Therefore, the stresses σ_{13}^q and σ_{23}^q defined in equation (2) follow from equation (23) as follows

$$\sigma_{13}^q(x, y, t) = ik\mu_q \sum_{m=1}^{\infty} \left(\frac{\alpha_m R_m \cosh\left(\frac{\alpha_m}{2\mu_q} t\right) + M_m \sinh\left(\frac{\alpha_m}{2\mu_q} t\right)}{\alpha_m} \right) \times X_{qm}(y) e^{ikx - \frac{\delta c_q^2}{2\mu_q} t},$$
$$\sigma_{23}^q(x, y, t) = \mu_q \sum_{m=1}^{\infty} \left(\frac{\alpha_m R_m \cosh\left(\frac{\alpha_m}{2\mu_q} t\right) + M_m \sinh\left(\frac{\alpha_m}{2\mu_q} t\right)}{\alpha_m} \right) \times X'_{qm}(y) e^{ikx - \frac{\delta c_q^2}{2\mu_q} t}, \tag{24}$$

for $q = c, s$. Also, the signs ($'$) and ($''$) denote the first and second derivatives, respectively.

3.2. Antisymmetric solutions

Here also, the antisymmetric solution for $y \geqslant 0$ from equation (14) takes the form

$$\begin{cases} X_{cm}(y) = B_2 \sin(y\sqrt{\lambda_m^2 - k^2}), \\ X_{sm}(y) = A_1 \cos(y\sqrt{\lambda_m^2 - k^2}) + B_1 \sin(y\sqrt{\lambda_m^2 - k^2}), \end{cases} \tag{25}$$

and yields the following solution matrix from the conditions given in equations (9)–(10)and the solutions in equation (25) as follows:

$$\begin{pmatrix} \cos(h_c\sqrt{\lambda_m^2 - k^2}) & \sin(h_c\sqrt{\lambda_m^2 - k^2}) & -\sin(h_c\sqrt{\lambda_m^2 - k^2}) \\ -\sin(h_c\sqrt{\lambda_m^2 - k^2}) & \cos(h_c\sqrt{\lambda_m^2 - k^2}) & -\frac{\mu_c}{\mu_s}\cos(h_c\sqrt{\lambda_m^2 - k^2}) \\ -\sin((h_c + h_s)\sqrt{\lambda_m^2 - k^2}) & \cos((h_c + h_s)\sqrt{\lambda_m^2 - k^2}) & 0 \end{pmatrix}, \tag{26}$$

that gives the following eigenwave equation

$$\tan(h_c\sqrt{\lambda_m^2 - k^2}) \tan(h_s\sqrt{\lambda_m^2 - k^2}) = \frac{\mu_c}{\mu_s}. \tag{27}$$

Thus from equation (27), explicit solution of the eigenvalues λ_m cannot be obtained analytically, but numerically or by other means [28]. To analyze further, we set $k = 0$ to get the global lower eigenvalues range for $\lambda_m \ll 1$ and reveals

$$\frac{\mu_c}{\mu_s} \ll \frac{h_s}{h_c} \ll \left(\frac{\mu_c}{\mu_s}\right)^{-1}. \tag{28}$$

Also for the eigenfunctions, the solutions given in equation (25) via the conditions in equations (9)–(10) are revealed to be as follows:

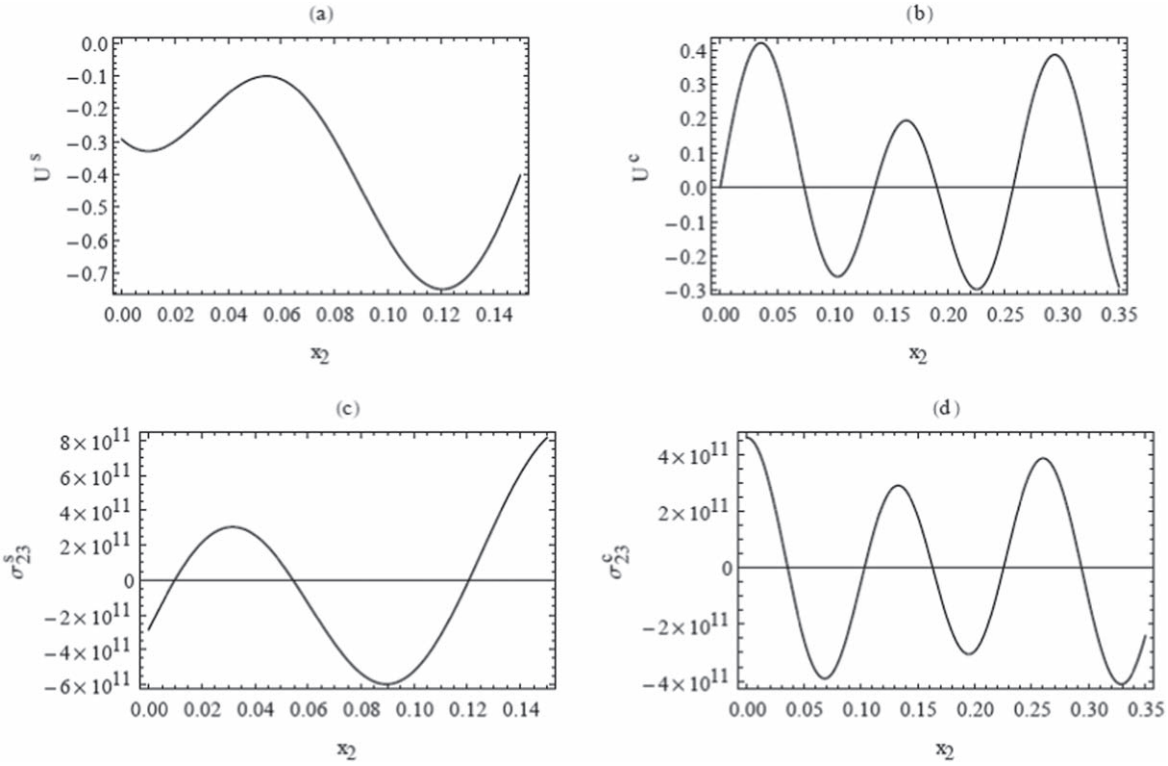

Figure 2. Curves for the free undamped displacements of the skin (a) and core (b) layers and free undamped stresses of the skin (c) and core (d) layers in equation (38).

$$\begin{cases} X_{cm}(y) = \sin\left(y\sqrt{\lambda_m^2 - k^2}\right), \\ X_{sm}(y) = B_{2m}\left(\cos\left(y\sqrt{\lambda_m^2 - k^2}\right) + \tan\left((h_c + h_s)\sqrt{\lambda_m^2 - k^2}\right)\sin\left(y\sqrt{\lambda_m^2 - k^2}\right)\right), \end{cases} \tag{29}$$

where

$$B_{2m} = \frac{\sin\left(h_c\sqrt{\lambda_m^2 - k^2}\right)}{\cos\left(h_c\sqrt{\lambda_m^2 - k^2}\right) + \sin\left(h_c\sqrt{\lambda_m^2 - k^2}\right)\tan\left((h_c + h_s)\sqrt{\lambda_m^2 - k^2}\right)}. \tag{30}$$

Now, to determine the function $T_{qm}(t)$, we substitute equation (12) with the help of equation (13) into equation (8) and the initial conditions given in equation (11) to get the following differential equations:

$$\begin{cases} T''_{qm}(t) + \frac{\delta c_q^2}{\mu_q} T'_{qm}(t) + (c_q\lambda_m)^2 T_{qm}(t) = 0, \\ T_{qm}(0) = R_m, \quad T'_{qm}(0) = N_m, \end{cases} \tag{31}$$

for $q = c, s$,where R_m and N_m are given by the application of the Fourier's series as

$$R_m = \frac{\int_0^{h_c} f_c(\xi_2)X_{cm}(\xi_2)d\xi_2 + \int_{h_c}^{h_s} f_s(\xi_2)X_{sm}(\xi_2)d\xi_2}{\int_0^{h_c} X_{cm}^2(\xi_2)d\xi_2 + \int_{h_c}^{h_s} X_{sm}^2(\xi_2)d\xi_2},$$
$$N_m = \frac{\int_0^{h_c} g_c(\xi_2)X_{cm}(\xi_2)d\xi_2 + \int_{h_c}^{h_s} g_s(\xi_2)X_{sm}(\xi_2)d\xi_2}{\int_0^{h_c} X_{cm}^2(\xi_2)d\xi_2 + \int_{h_c}^{h_s} X_{sm}^2(\xi_2)d\xi_2}, \tag{32}$$

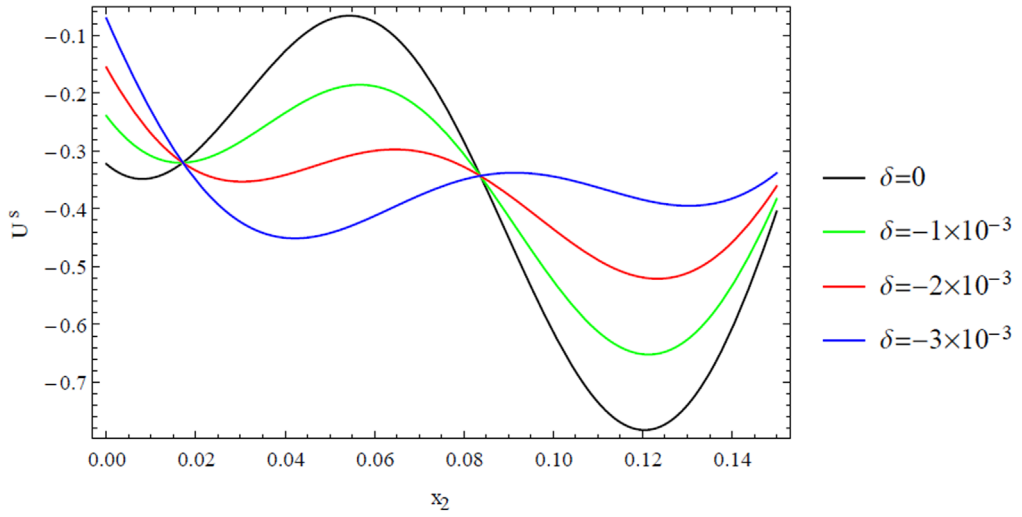

Figure 3. Curves for the underdamped displacement of the skin layer in equation (40) with various δ values.

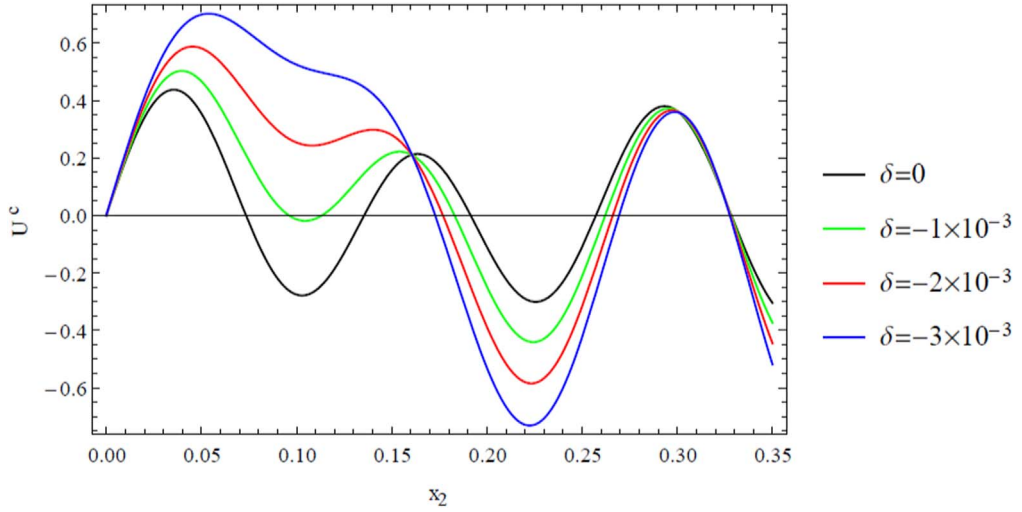

Figure 4. Curves for the underdamped displacement of the core layer in equation (40) with various δ values.

with X_{qm} (y), $(q = c, s)$ in equation (29). Also. the solutions of equations (31) are given by

$$T_{qm}(t) = \frac{\alpha_m R_m \cosh\left(\frac{\alpha_m}{2\mu_q}t\right) + M_m \sinh\left(\frac{\alpha_m}{2\mu_q}t\right)}{\alpha_m} e^{-\frac{\delta c_q^2}{2\mu_q}t}, \tag{33}$$

where $M_m = 2\mu_q N_m + \delta c_q^2 R_m$ and $\alpha_m = \sqrt{c_q^4\delta^2 - 4\mu_q c_q^2 \lambda_m^2}$.

Therefore, from the assumptions made at the beginning of this section and via equations (12) and (33) we get the complete out of plane displacements in the respective layers as

$$U^q(x, y, t) = \sum_{m=1}^{\infty}\left(\frac{\alpha_m R_m \cosh\left(\frac{\alpha_m}{2\mu_q}t\right) + M_m \sinh\left(\frac{\alpha_m}{2\mu_q}t\right)}{\alpha_m}\right) \times X_{qm}(y) e^{ikx - \frac{\delta c_q^2}{2\mu_q}t}, \quad q = c, s, \tag{34}$$

where $X_{qm}(y)$ are given in equation (29), and R_m and N_m in equation (32).

The stresses σ_{13}^q and σ_{23}^q also follow from equation (34) are as follows

$$\begin{aligned}
&\sigma_{13}^q(x, y, t) \\
&= ik\mu_q \sum_{m=1}^{\infty}\left(\frac{\alpha_m R_m \cosh\left(\frac{\alpha_m}{2\mu_q}t\right) + M_m \sinh\left(\frac{\alpha_m}{2\mu_q}t\right)}{\alpha_m}\right) \\
&\quad \times X_{qm}(y) e^{ikx - \frac{\delta c_q^2}{2\mu_q}t}, \\
&\sigma_{23}^q(x, y, t) \\
&= \mu_q \sum_{m=1}^{\infty}\left(\frac{\alpha_m R_m \cosh\left(\frac{\alpha_m}{2\mu_q}t\right) + M_m \sinh\left(\frac{\alpha_m}{2\mu_q}t\right)}{\alpha_m}\right) \\
&\quad \times X'_{qm}(y) e^{ikx - \frac{\delta c_q^2}{2\mu_q}t},
\end{aligned} \tag{35}$$

for $q = c, s$.

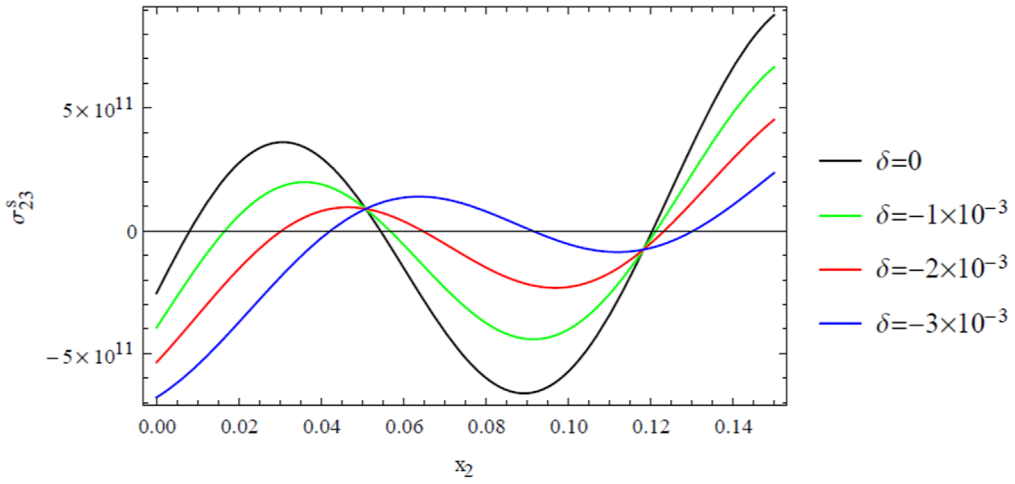

Figure 5. Curves for the underdamped stress of the skin layer in equation (40) with various δ values.

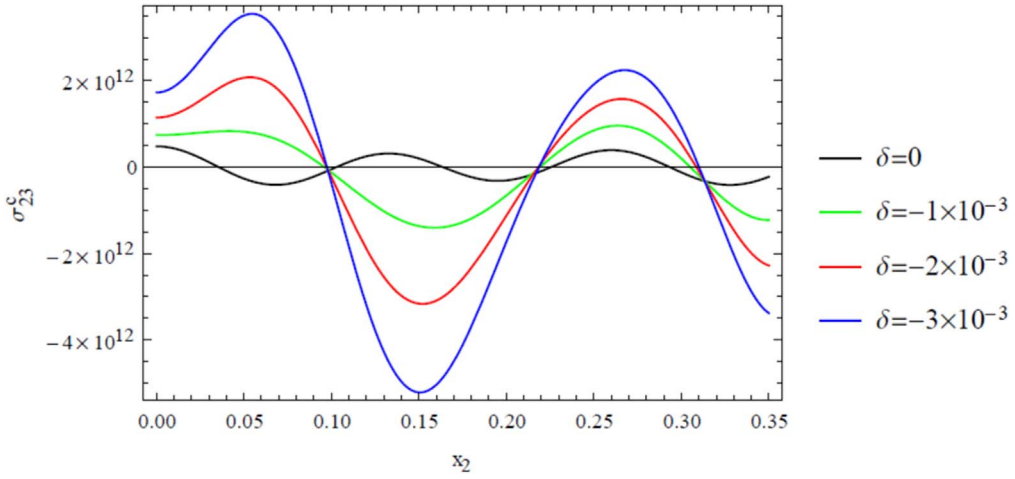

Figure 6. Curves for the underdamped stress of the skin layer in equation (40) with various δ values.

4. Analysis of the solutions

In this section, we analyze the effects of the viscous damping parameter δ on the closed form solutions of the out of plane displacements and the stresses determined. In doing so, we consider the antisymmetric solutions having possessed a global lower eigenvalues range as estimated in equation (28) and also due to the fact that it is more practical in the plate theory. Note that similar analysis can also be carried out in regard to the symmetric solutions. Thus, considering the antisymmetric solutions given in equations (34)–(35) couple to equation (29) and equation (32) for R_m and N_m, we therefore rewrite equations (34)–(35) as follow [26]

$$\begin{aligned}
U^q(x,y,t) &= \sum_{m=1}^{\infty}\left(\frac{\beta_{qm}R_m\cosh\left(\omega_{qm}t\sqrt{\xi_{qm}^2-1}\right)+M_m\sinh\left(\omega_{qm}t\sqrt{\xi_{qm}^2-1}\right)}{\beta_{qm}}\right)\\
&\quad\times X_{qm}(y)e^{ikx-c_q\xi_{qm}t},\\
\sigma^q_{13}(x,y,t) &= ik\mu_q\sum_{m=1}^{\infty}\left(\frac{\beta_{qm}R_m\cosh\left(\omega_{qm}t\sqrt{\xi_{qm}^2-1}\right)+M_m\sinh\left(\omega_{qm}t\sqrt{\xi_{qm}^2-1}\right)}{\beta_{qm}}\right)\\
&\quad\times X_{qm}(y)e^{ikx-c_q\xi_{qm}t},\\
\sigma^q_{23}(x,y,t) &= \mu_q\sum_{m=1}^{\infty}\left(\frac{\beta_{qm}R_m\cosh\left(\omega_{qm}t\sqrt{\xi_{qm}^2-1}\right)+M_m\sinh\left(\omega_{qm}t\sqrt{\xi_{qm}^2-1}\right)}{\beta_{qm}}\right)\\
&\quad\times X'_{qm}(y)e^{ikx-c_q\xi_{qm}t},
\end{aligned}\tag{36}$$

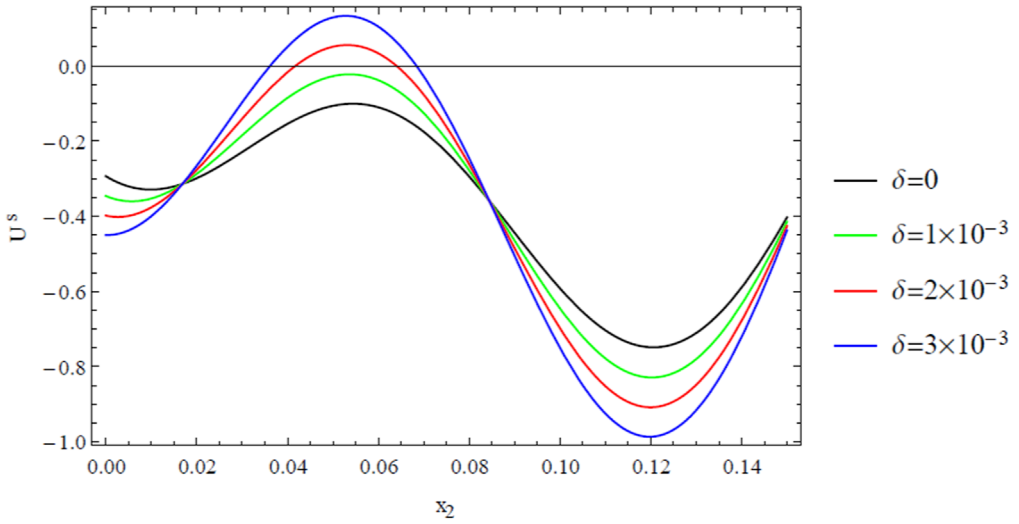

Figure 7. Curves for the overdamped displacement of the skin layer in equation (41) with various δ values.

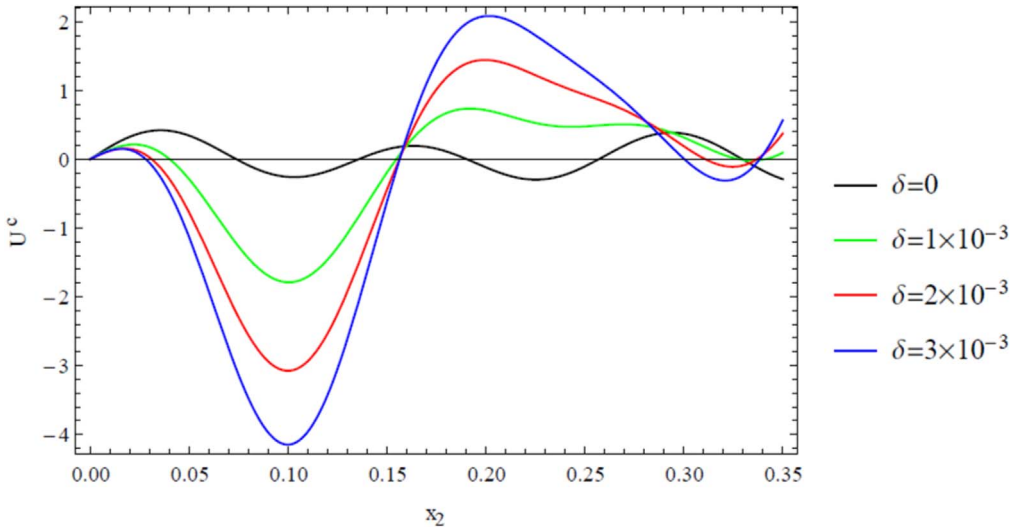

Figure 8. Curves for the overdamped displacement of the core layer in equation (41) with various δ values.

also for $q = c, s$, and

$$\omega_{qm} = c_q \lambda_m, \quad \xi_{qm} = \frac{\delta}{D_{qm}},$$
$$D_{qm} = \frac{2\mu_q \lambda_m}{c_q}, \quad \beta_{qm} = 2\mu_q \sqrt{\xi_{qm}^2 - 1}. \tag{37}$$

We therefore analyze the above displacements and stresses by considering the following cases of free undamped and free damped situations, respectively:

4.1. Free undamped quantities $\xi_{qm} = 0$ $(\delta = 0)$

To obtain the free undamped displacements and stresses, we set $\xi_{qm} = 0$ $(\delta = 0)$ in equation (34)–(35) to get the following:

$$U^q(x, y, t) = \sum_{m=1}^{\infty} (R_m \cos(\omega_{qm} t) + N_m \sin(\omega_{qm} t)) X_{qm}(y) e^{ikx},$$
$$\sigma_{13}^q(x, y, t) = ik\mu_q \sum_{m=1}^{\infty} (R_m \cos(\omega_{qm} t) + N_m \sin(\omega_{qm} t)) X_{qm}(y) e^{ikx},$$
$$\sigma_{23}^q(x, y, t) = \mu_q \sum_{m=1}^{\infty} (R_m \cos(\omega_{qm} t) + N_m \sin(\omega_{qm} t)) X'_{qm}(y) e^{ikx}, \tag{38}$$

for $q = c, s$.

4.2. Critically damped quantities $\xi_{qm} = 1$

For the critically damped quantities, we set $\xi_{qm} = 1$ in equation (34)–(35) to obtain the following:

$$\begin{aligned} U^q(x, y, t) &= \sum_{m=1}^{\infty} R_m X_{qm}(y) e^{ikx - c_q t}, \\ \sigma_{13}^q(x, y, t) &= ik\mu_q \sum_{m=1}^{\infty} R_m X_{qm}(y) e^{ikx - c_q t}, \\ \sigma_{23}^q(x, y, t) &= \mu_q \sum_{m=1}^{\infty} R_m X'_{qm}(y) e^{ikx - c_q t}, \end{aligned} \tag{39}$$

for $q = c, s$.

4.3. Underdamped quantities $\xi_{qm} < 1$

Finallyfor underdamped displacements and stresses, we consider the state where $\xi_{qm} < 1$ $(\delta < 1)$ in equations (34)–(35) to get the following:

$$\begin{aligned} U^q(x, y, t) &= \sum_{m=1}^{\infty} \left(\frac{\gamma_{qm} R_m \cos(\omega_{qm} t\sqrt{1 - \xi_{qm}^2}) + M_m \sin(\omega_{qm} t\sqrt{1 - \xi_{qm}^2})}{\gamma_{qm}} \right) \\ &\quad \times X_{qm}(y) e^{ikx - c_q \xi_{qm} t}, \\ \sigma_{13}^q(x, y, t) &= ik\mu_q \sum_{m=1}^{\infty} \left(\frac{\gamma_{qm} R_m \cos(\omega_{qm} t\sqrt{1 - \xi_{qm}^2}) + M_m \sin(\omega_{qm} t\sqrt{1 - \xi_{qm}^2})}{\gamma_{qm}} \right) \\ &\quad \times X_{qm}(y) e^{ikx - c_q \xi_{qm} t}, \\ \sigma_{23}^q(x, y, t) &= \mu_q \sum_{m=1}^{\infty} \left(\frac{\gamma_{qm} R_m \cos(\omega_{qm} t\sqrt{1 - \xi_{qm}^2}) + M_m \sin(\omega_{qm} t\sqrt{1 - \xi_{qm}^2})}{\gamma_{qm}} \right) \\ &\quad \times X'_{qm}(y) e^{ikx - c_q \xi_{qm} t}, \end{aligned} \tag{40}$$

for $q = c, s$, and where $\gamma_{qm} = 2\mu_{qm}\sqrt{1 - \xi_{qm}^2}$.

4.4. Overdamped quantities $\xi_{qm} > 1$

For the overdamped displacements and stresses, we consider the situation when $\xi_{qm} > 1 (\delta > 1)$ in equation (34)–(35) to get the following:

$$\begin{aligned} U^q(x, y, t) &= \sum_{m=1}^{\infty} \left(\frac{\beta_{qm} R_m \cosh(\omega_{qm} t\sqrt{\xi_{qm}^2 - 1}) + M_m \sinh(\omega_{qm} t\sqrt{\xi_{qm}^2 - 1})}{\beta_{qm}} \right) \\ &\quad \times X_{qm}(y) e^{ikx - c_q \xi_{qm} t}, \\ \sigma_{13}^q(x, y, t) &= ik\mu_q \sum_{m=1}^{\infty} \left(\frac{\beta_{qm} R_m \cosh(\omega_{qm} t\sqrt{\xi_{qm}^2 - 1}) + M_m \sinh(\omega_{qm} t\sqrt{\xi_{qm}^2 - 1})}{\beta_{qm}} \right) \\ &\quad \times X_{qm}(y) e^{ikx - c_q \xi_{qm} t}, \\ \sigma_{23}^q(x, y, t) &= \mu_q \sum_{m=1}^{\infty} \left(\frac{\beta_{qm} R_m \cosh(\omega_{qm} t\sqrt{\xi_{qm}^2 - 1}) + M_m \sinh(\omega_{qm} t\sqrt{\xi_{qm}^2 - 1})}{\beta_{qm}} \right) \\ &\quad \times X'_{qm}(y) e^{ikx - c_q \xi_{qm} t}, \end{aligned} \tag{41}$$

for $q = c, s$.

5. Numerical results and discussion

The present section gives the numerical result and discussions of the formulated problem. In doing so, the overall plate is considered to be a sandwich plate of length 1 m, composed of an upper skin layer made of copper material of length 0.15 m, a core layer made of aluminum material of length 0.7 m and a lower skin layer made of copper material of length 0.15 m, just as shown in figure 1. Since the plate is symmetrical around $y = 0$, we consider half of the plate since we analyze the antisymmetric solution as explained in the above section. Thus, we have the following values for the dimensional lengths and wave number: $h_s = 0.15$, $h_c = 0.35$ and k=1.

We also consider the following initial data in the respective skin and core layers:

$$f_c(y) = 2y, \ f_s(y) = 10y, \ g_c(y) = \sin(y), \ g_s(y) = \cos(y), \tag{42}$$

For the skin layer, we take the relevant elastic parameters for copper material [29] as follows:

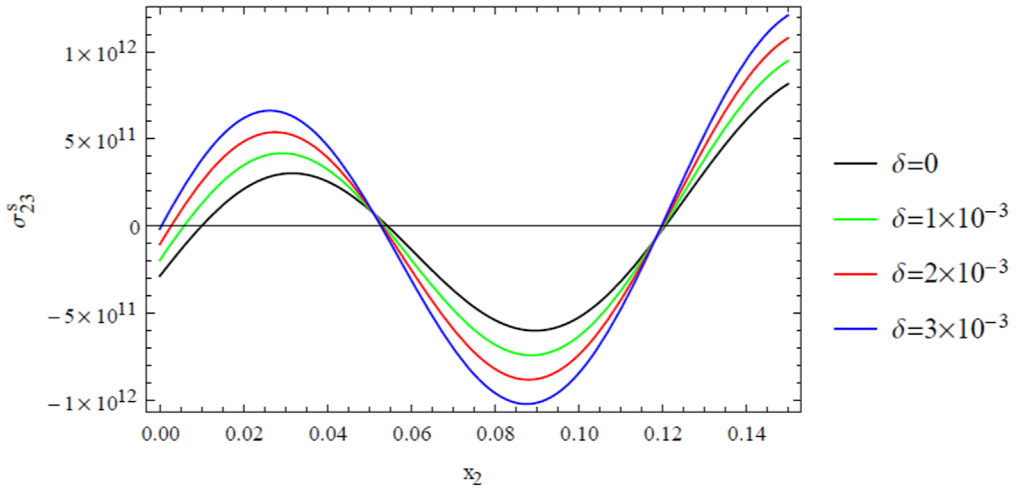

Figure 9. Curves for the overdamped stress of the skin layer in equation (41) with various δ values.

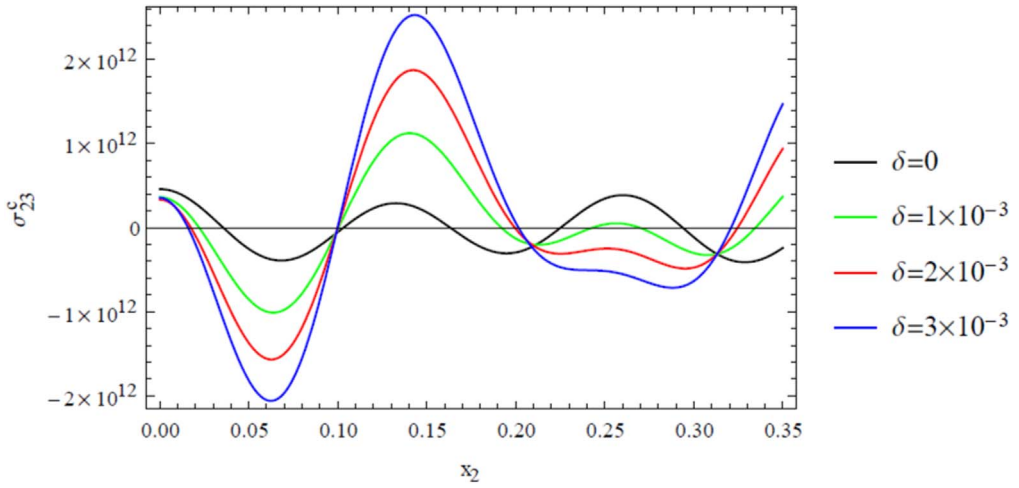

Figure 10. Curves for the overdamped stress of the core layer in equation (41) with various δ values.

$$\mu_s = 3.86 \times 10^{10} Pa, \quad \rho_s = 8.954 \times 10^3 Kgm^{-3}, \tag{43}$$

also for the core layer, we take aluminum material with the following elastic parameters [30]:

$$\mu_c = 2.46 \times 10^{10} Pa, \quad \rho_c = 2.66 \times 10^3 Kgm^{-3}. \tag{44}$$

Furthermore, we have made use of c_q as μ_q/ρ_q in the numerical computation for our convenience. Also, since our method requires eigenvalues, we compute the first five eigenvalues using the above data, via bisection numerical method [28] as follows:

$$\lambda_1 = 49.378, \quad \lambda_2 = 46.6896, \quad \lambda_3 = 34.9133, \\ \lambda_4 = 27.9507, \quad \lambda_5 = 16.1838. \tag{45}$$

Various dimensional displacement and shear stress plots have been depicted below taking in to account the variations or effects of the viscous damping parameter δ on the propagation of Rayleigh waves in the plate under consideration. We give the two-dimensional plots for the free damped and free undamped cases in figures 2–10. Furthermore, before we go into detailed discussion, it is important to remember here that the skin and core layers are assumed to be of different lengths, thus mere comparison by looking at the two respective graphs of the core and skin layers may be tempting. Further, it is vital to note that the chosen initial conditions in the respective layers play significant role in the nature of the wave propagation profile as rightly asserted by D'Alembert [1, 26].

Figure 2 portrays various curves for the wave displacements of the skin (a) and core (b) layers, and shear stresses σ_{23} of the skin (c) and core (d) layers given in equation (38) in the absence of viscous damping, that is when $\xi_{qm} = 0$ ($\delta = 0$). Propagation occurred periodically with varying wavelengths and dissimilar amplitudes. In both quantities, it is noted that the travelling amplitudes in the case of skin layer are higher than that of the core layer; while opposite trend is noted in the case of wavelengths. Of course this could results from the fact that the stiffness in the skin layer μ_s is higher than that of the core layer μ_c.

Figure 3 shows the variation of the displacement profile of the skin layer given in equation (40) with respect to the space variable y for various values of viscous damping parameter δ. The undamped displacement which appears when $\delta = 0$ has the highest amplitude, and then follows with

underdamped profiles when $\delta < 0$. It can be observed here that the undamped displacement profile in the presence of damping is maintained till $\delta = -2 \times 10^{-3}$, and then begins to change greatly. Similar interpretation goes to figure 4 for the variation of the displacement profile of the core layer given in equation (40); where the damping effect is more significant in the internal $0.01 \leqslant y \leqslant 0.16$ and then continues smoothly.

In figure 5, the variation of the shear stress σ_{23}^{s} profile of the skin layer given in equation (40) with respect to the space variable y for various underdamped values are shown. Also, it is noticed that the profile begins to be affected greatly for $\delta < -2 \times 10^{-3}$ as is seen in the interval $0.05 \leqslant y \leqslant 0.118$. Comparably, similar interpretation goes to figure 6 for the variation of the shear stress σ_{23}^{c} of the core layer given in equation (39) with more sensitive region comprising of $0.00 \leqslant y \leqslant 0.217$.

Figures 7 and 8 depict the variations of the displacement profiles of the skin and core layers given in equation (41) with respect to the space variable y for various values of overdamped parameter δ. The displacement profiles in the case of skin layer are not much disturbed in comparison with that of the core layer that struggle to maintain the periodic movement form in the presence of overdamping.

Finally, figures 9 and 10 illustrate the variations of the shear stress profiles of the skin σ_{23}^{s} and core σ_{23}^{c} layers given in equation (41) with respect to the space variable y for various values of overdamped parameter δ. Periodicity in the stress profile is maintained in the skin layer despite the variation in δ; while significant deviation is noted in the core layer amidst different values of δ.

6. Conclusion

In conclusion, effects of viscous damping on the propagation of anti-plane Rayleigh waves in an elastic three-layered inhomogeneous plate have been investigated. The layers of the plate are considered to be of homogenous isotropic materials of different material properties, and are bounded together with perfect interfacial conditions and traction-free boundary conditions on the outer faces of the skin layers. The eigenfunctions expansion method is employed for the study and the antisymmetric solution modes have been completely analyzed amidst free damped and undamped situations. Furthermore, a 1 m symmetric plate made of aluminium core layer and copper skin layers is considered for the numerical computations, of which a bisection method is utilized for the computations of the first five eigenvalues. Finally, it is noted that the effects of viscous damping on the propagation of Rayleigh waves in a layered plate is significant looking at the variations in the displacement and shear stress for very small amount of damping (as small as $10^{\pm 4}$ for core layer and $10^{\pm 5}$ for skin layers). Also, the damping effect is noted to be more visible in the core layer, which is due to the fact that the material stiffness there is less than that of the skin layer.

It is summarized that the above consideration can be utilized in furthering the study of damping effects on multilayered elastic structures which have been investigated in the literature due to their various applications such as in sandwich plates, layered laminates, automotive industries, modern aerospace, photovoltaic panels and beams considerations.

Acknowledgments

The first author, Rahmatullah Ibrahim Nuruddeen sincerely acknowledges the 2017 CIIT-TWAS Full-time Postgraduate Fellowship Award (FR Number: 3 240 299 480).

References

[1] Achenbach J D 1999 *Wave Propagation in Elastic solids, Eight Impression* (Netherland: Elsevier)
[2] Kaplunov J D, Kossovich L Y and Nolde E V 1998 *Dynamics of Thin Walled Elastic Bodies* (San Diego, CA: Academic)
[3] Andrianov I V, Awrejcewicz J, Danishevs'kyy V V and Ivankov O A 2014 *Asymtotic Methods in the Theory of Plates with Mixed Boundary Conditions* (UK: John Wiley & Sons, Ltd.)
[4] Kaplunov J and Nobili A 2017 *Math. Methods Appl. Sci.* **40** 3381
[5] Craster R, Joseph L and Kaplunov J 2014 *Wave Motion* **51** 581
[6] Sayyad A S and Ghugal Y M 2017 *Compos. Struct.* **171** 486
[7] Sahin O, Erbas B, Kaplunov J and Savsek T 2019 *Arch. Appl. Mech.* **90** 339–52
[8] Altenbach H, Eremeyev V A and Naumenko K 2015 *ZAMM* **95** 1004
[9] Naumenko K and Eremeyev V A 2014 *Compos. Struct.* **112** 283
[10] Shishehsaz M, Raissi H and Moradi S 2019 *Mechanics Adv. Materials Struct.* **26** 1234
[11] Lee P and Chang N 1979 *J. Elasticity* **9** 51
[12] Kaplunov J, Prikazchikov D and Prikazchikova L 2017 *Int. J. Solids Struct.* **113** 169
[13] Kaplunov J, Prikazchikov D A and Sergushova O 2016 *J. Sound Vib.* **366** 264
[14] Zhai Y, Li Y and Liang S 2018 *Solids Struct.* **200** 346
[15] Lopez-Aenlle M and Pelayo F 2019 *Solids Struct.* **212** 259
[16] Satti J U, Afzal M and Nawaz R 2019 *Phys. Scr.* **94** 115223
[17] Demirkus D 2018 *Z. Angew. Math. Phys.* **69** 69
[18] Demirkus D 2018 *Int. J. Non-Linear Mechanics* **102** 53
[19] Ayub M, Naeem A and Nawaz R 2010 *Phys. Scr.* **82** 4
[20] Lotfy K and El-Bary A A 2019 *Iranian J. Sci. Techn.: Trans. Mech. Eng.* (https://doi.org/10.1007/s40997-019-00315-x)
[21] Lotfy K and Hassan W 2016 *Preprints* 2016070017
[22] Belarbi M O, Tati A, Ounis H and Khechai A 2017 *Latin American J. Solids Struc.* **14** 2265
[23] Berdichevsky V L 2010 *Int. J. Eng. Sci.* **48** 383
[24] Prikazchikov L A, Aydin Y E, Erbas B and Kaplunov J 2018 *Math. Mechanics Solids* **25** 3–16
[25] Erbas B 2018 *Eskisehir Techn. University J. Sci. Techno., A-Appl. Sci. Eng.* **19** 867
[26] Leissa A W and Qatu M S 2011 *Vibrations of Continous Systems* (U.S.A: McGraw Hill Companies Inc.) 978-0-07-145728-6
[27] Abbas I A 2014 *Comp. Math. Appl.* **68** 2036
[28] Ozisik M N 1980 *Heat Conduction* (New York: Wiley Interscience)
[29] Abo-Dahab S M, Lotfy K and Gohaly A 2015 *Math. Probl. Eng.* **2015** 671783
[30] Anya A I, Akhtar M W, Abo-Dahab S M, Kaneez H, Khan A and Jahangir A 2018 *J. Mech. Behavior Mat.* **2018** 2018–0002